USE OF CRYSTALS IN BALANCED MIXERS *

Jesse Taub and Paul J. Giordano
U. S. Naval Material Laboratory
N. Y. Naval Shipyard
Brooklyn, N. Y.

Summary

The crystal parameters to be considered for obtaining accurate information about local oscillator noise suppression in a balanced mixer are theoretically presented. The interrelationship between available local oscillator noise suppression and the important design characteristics of microwave receivers are discussed and curves are plotted. A method of accurately measuring local oscillator noise suppression is given and experimental data is correlated with theoretical results.

Introduction

It is generally known that the degree of local oscillator noise suppression obtainable in a balanced microwave mixer is dependent on the parameters of the crystal pair employed, and that a "matched pair" will give better local oscillator noise suppression than a pair whose parameters differ. Although there has been some literature[1,2] on the effect of conversion loss and IF impedance unbalance, there has been no quantitative presentation of the effect of rf impedance, IF impedance, and conversion loss simultaneously. This paper deals with this theory in a more rigorous fashion. In so doing, it is hoped that many of the prevalent misconceptions as to what constitutes a "matched pair" will be eliminated. Having a more quantitative knowledge of the effect of crystal parameter unbalance on local oscillator noise suppression will enable the receiver designer to exercise greater control of balanced mixer performance. This should result in receivers of lower and more uniform noise figures.

1. Analysis of rf Portion of Balanced Mixer

In order to arrive at suitable equations for determining local oscillator noise suppression an analysis of the rf portion of a balanced mixer is given in Fig. 1.

The rf admittances of the crystals in arms 1 and 2 of the magic tee balanced mixer shown in Fig. 1 can be represented by normalized conductances g_1 and g_2 and line lengths l_1 and l_2. The phase of the admittances are thus lumped with l_1 and l_2. The incident voltages on crystals 1 and 2 due to the local oscillator will be

* The opinions or assertions contained in this paper are the private ones of the author and are not to be construed as official, or reflecting the views of the Navy Department or the Naval Service at large.

1 R. Pound, "Microwave Mixers," McGraw-Hill Book Co., New York, ch. 6; 1948.

2 TRE Technical Memorandum no. 67.

$$V_{i_{L_1}} = R_e \frac{V_{i_L}}{\sqrt{2}} \varepsilon^{j\omega_L t} \varepsilon^{-j\beta_L \ell_1} \tag{1a}$$

and

$$V_{i_{L_2}} = R_e \frac{V_{i_L}}{\sqrt{2}} \varepsilon^{j\omega_L t} \varepsilon^{-j\beta_L \ell_2} \tag{1b}$$

where ω_L is the local oscillator radian frequency and β_L is the propagation constant at the local oscillator frequency. Due to mismatch in each arm, the effective rf voltage across the crystal differs from the incident voltage by a real constant. These voltages are

$$V_{t_{L_1}} = K_1 R_e \varepsilon^{j(\omega_L t - \beta_L \ell_1)} \tag{2a}$$

and

$$V_{t_{L_2}} = K_2 R_e \varepsilon^{j(\omega_L t - \beta_L \ell_2)} \tag{2b}$$

where

$$K_1 = \frac{\sqrt{2}\, V_{i_L}}{1 + g_1} \quad \text{and} \quad K_2 = \frac{\sqrt{2}\, V_{i_L}}{1 + g_2}$$

Similarly, an incident signal voltage V_{i_s} fed through the E plane arm would produce at the crystal terminals

$$V_{i_{s_1}} = C_1 R_e \varepsilon^{j(\omega_s t + \phi - \beta_s \ell_1)} \tag{3a}$$

and

$$V_{i_{s_2}} = -C_2 R_e \varepsilon^{j(\omega_s t + \phi - \beta_s \ell_2)} \tag{3b}$$

where

$$C_1 = \frac{\sqrt{2}\, V_{i_s}}{1 + g_1}, \quad C_2 = \frac{\sqrt{2}\, V_{i_s}}{1 + g_2}$$

and ϕ represents the shift in the time zero relative to the local oscillator wave. In order to compute the resulting IF output voltages from the two mixer arms, the assumption of square law mixing is made. Thus, the resulting output voltages would be

$$V_{o_1} = A (V_{i_{L_1}} + V_{i_{s_1}})^2 \tag{4a}$$

and $$V_{o_2} = B\,(V_{i_{L_2}} + V_{i_{s_2}})^2 \tag{4b}$$

Substituting (2a) and (3a) in (4a), (2b) and (3b) in (4b), and only considering the terms that are functions of $\omega_S - \omega_L$ gives

$$V_{i_{f_1}} = C_1K_1 \cos\left[(\omega_s - \omega_L)t + \phi + (\beta_L - \beta_s)\ell_1\right] \tag{5a}$$

and

$$V_{i_{f_2}} = -C_2K_2 \cos\left[(\omega_s - \omega_L)t + \phi + (\beta_L - \beta_s)\ell_2\right] \tag{5b}$$

Since $(\beta_L - \beta_S)(\ell_2 - \ell_1)$ is at most 3° for wavelengths of 10 cm and below and is usually much less, it is seen from (5a) and (5b) that V_{if_2} is very nearly 180° out of phase with V_{if_1} independent of the phase of the rf admittances of the crystals. A similar analysis for the local oscillator noise mixing with the local oscillator would yield two IF noise voltages that are very nearly in phase.

2. Noise Suppression Equations

From the above analysis the equations for CK for a crystal is proportional to the square root of its conversion loss, where conversion loss is defined as including the mismatch loss. Thus, in a hybrid coil type of coupling circuit the resultant output signal voltage is

$$V_+ = C_1K_1 + C_2K_2 = \sqrt{L_1} + \sqrt{L_2} \tag{6}$$

If this voltage were to be suppressed, it would be equal to

$$V_- = \sqrt{L_1} - \sqrt{L_2} \tag{7}$$

The noise suppression, thus, becomes

$$S = \left(\frac{V_+}{V_-}\right)^2 = \left(\frac{\sqrt{L_1} + \sqrt{L_2}}{\sqrt{L_1} - \sqrt{L_2}}\right)^2 \tag{8}$$

For the non-hybrid IF coupling circuit used in most receivers, the considerations are slightly different. In the parallel feed circuit of Fig. 2, e_1 and e_2 are the equivalent open circuit IF voltages of each mixer arm and $R_{i_{f_1}}$ and $R_{i_{f_2}}$ their IF resistance.

It is assumed that all reactances are neutralized. Taking the square of the ratio of in-phase and antiphase output voltages, gives:

$$S = \left(\frac{\frac{e_1}{R_{if_1}} + \frac{e_2}{R_{if_2}}}{\frac{e_1}{R_{if_1}} - \frac{e_2}{R_{if_2}}} \right)^2 \tag{9}$$

where $\frac{e_1}{R_{if_1}}$ and $\frac{e_2}{R_{if_2}}$

are the short circuit IF currents of the two crystals. Since the conversion loss is proportional to the square of the IF output voltage developed by the crystal across a standard load resistance (400 + j0 for the 1N23B), e can be related to the conversion loss in the manner depicted in Fig. 3.

$$e = E_b \frac{(R_L + R_{if})}{R_L} = E_b \left(1 + \frac{R_{if}}{R_L}\right)$$

$$e = K \sqrt{L} \left(1 + \frac{R_{if}}{R_L}\right) \tag{10}$$

In order to easily determine conversion loss and IF impedance unbalance limits for a given noise suppression, Eq. (9), which can be written as

$$S_{db} = 10 \log \left(\frac{1 + a}{1 - a}\right)^2 \tag{11}$$

where

$$a = \frac{e_1 R_{if_2}}{e_2 R_{if_1}} = \frac{\sqrt{L_1}}{\sqrt{L_2}} \frac{R_{if_2}}{R_{if_1}} \frac{(R_{if_1} + R_o)}{(R_{if_2} + R_o)}$$

was plotted in Fig. 4. In the above equation, R_o is the average IF impedance of the crystal. Fig. 4 is a plot of local oscillator noise suppression in db as a function of db unbalance in conversion loss with IF impedance unbalance factor

$$\left[\frac{R_{if_2}}{R_{if_1}} \frac{(R_{if_1} + R_o)}{(R_{if_2} + R_o)} \right]$$

as a parameter. It is seen from these curves that 20 db suppression can be achieved with 1.0 db of conversion loss unbalance and an IF impedance unbalance factor of 0.9. The IF impedance limits can be calculated from the value of the unbalance factor by using an approximation of this factor equal to

$$1 + \frac{R_{if_2} - R_{if_1}}{2\,R_o}$$

This is a good approximation when $R_{if_2} - R_{if_1}$ is small compared to R_o.

3. Receiver Noise Figure

The increase in receiver noise figure due to local oscillator noise is given by

$$F_{N_{db}} = 10 \log_{10} \left(1 + \frac{t'}{F_{i_f} + t - 1}\right) \tag{12}$$

where t' is the increase in apparent crystal noise temperature due to local oscillator noise. F_{if} is the effective IF noise figure, and t is the crystal noise temperature. If a balanced mixer of noise suppression S is employed, F_N becomes

$$F_{N_{db}} = 10 \log_{10} \left(1 + \frac{t'/s}{F_{i_f} + t - 1}\right) \tag{13}$$

Since it is desirable to have F_N well under 1 db, $\frac{t'/s}{F_{i_f} + t - 1}$ must be much smaller than 1; therefore,

$$F_{N_{db}} \approx \frac{4.4\,t'/s}{F_{i_f} + t - 1} \tag{14}$$

Data compiled by P. D. Strum of Airborne Instruments Laboratory shows that the excess local oscillator noise ratio $(t' - 1)$ is proportional to the local oscillator frequency. These data for the side of the reflector mode exhibiting highest klystron noise are given in Table I.

TABLE I. KLYSTRON NOISE VERSUS LOCAL OSCILLATOR FREQUENCY (F_{if} = 30 mc)

Frequency	t'
3000	4.2
9375	10.5
16000	17.1
24000	25.0
35000	35.0

Substituting the data of Table I in Eq. (14), a family of curves was plotted for the db of noise suppression required to give 0.2 db receiver noise figure deterioration as a function of frequency with $(t - 1 + F_{if})$ as a parameter. Similar curves were also plotted for $\Delta F_{Ndb} = 0.3$ db and 0.4 db. These graphs are shown in Figs. 5, 6 and 7, respectively. It is readily seen that these curves can be useful in that they enable the receiver designer to quickly determine the degree of balanced mixer noise suppression required in terms of other design parameters.

4. Experimental Procedure

In order to verify the theoretical conclusions set forth it was necessary to obtain experimental correlation. The experimental approach decided upon was to measure the conversion loss, IF impedance, rf impedance, and crystal current for a large number of crystal pairs. These quantities were measured using standard measurement techniques. With this data, the theoretical noise suppression was calculated for each pair. Using a balanced mixer receiver, the actual noise suppression was measured and correlation with the theoretical results was studied. The measurement techniques for determining local oscillator noise suppression considered were:

a) The use of a fluorescent noise source in the local oscillator arm (coupled through a magic tee to avoid interaction of the local oscillator and noise signals) and the measurement of the change in noise figure with the noise source on and off. Noise suppression as a ratio then is

$$S = \frac{P}{\Delta F_N} \tag{15}$$

where P = the power ratio above KTB of the fluorescent noise source.

F_N = the difference in noise figure ratios for the two cases. This method gives an error for values of suppression greater than 10 db since the output power from the fluorescent noise source, which is initially small (12.86 db/KTB), when suppressed by more than 10 db, produces negligible change in noise figure ratio. This low output power, therefore, makes the fluorescent noise source unsuitable for local oscillator noise suppression measurements.

b) The use of a CW signal generator tuned to the signal frequency, and the injection of this signal alternately into the local oscillator and signal arms. The amount of added attenuation in the signal arm for the same receiver output reading is then a direct measure of the local oscillator noise suppression. In order to have stable operation, the frequency of the klystron signal generator must be 60 mc away from the local oscillator center frequency, and the frequency drift allowed is less than the bandwidth of the receiver. This degree of stability is difficult to obtain unless special stabilization circuits are employed.

c) In order to circumvent the difficulties inherent in (a) and in (b), a new technique was devised. This makes use of a signal source having the high power of a klystron and whose power spectrum simulates the effect of a fluorescent noise source. When a 2K25 klystron with sine wave modulation of the repeller electrode was employed, both of these desirable properties were obtained. If, for example,

the repeller is modulated at a 60 cycle rate ($f_q = 60$) and the maximum frequency deviation, f_d, is 6 mc, the components of the power spectrum will be

$$P_{(f)} \propto J_n^2 \ (X) \tag{16}$$

where X is equal to $\frac{f_d}{f_q}$ and

$$n = \frac{f}{f_q} \text{ , an integer.}$$

Since X is large for this case (10^5), the power spectrum can be approximated by:

$$P_{(f)} \propto \frac{2}{\pi X} \cos \left(X - \frac{2n + 1}{4} \pi\right) \tag{17}$$

provided $X >> n$.

Eq. (17), for its range of validity, predicts a power spectrum existing at 60 cycle intervals with only two repeating magnitudes. The exact spectrum would depend on X but for a given value of X the spectrum could resemble those shown in Fig. 8.

This proves that the frequency modulated wave used had a spectrum that would simulate, for the purpose of the noise suppression measurement, a white noise spectrum provided the bandwidth of the receiver is sufficiently small to keep $X >> n$. Since the system employed for determining local oscillator noise suppression measures the difference in the rf attenuation of the signal of the klystron when its output is shifted from the local oscillator arm to the signal arm, the absolute power level of that tube need not be known. The only limitation imposed upon this type of signal source is that its frequency modulated output power, within the bandwidth of the receiver, remain constant during the time required to make one measurement. The frequency deviation of this signal was much larger than the receiver bandwidth. Therefore, the small sample of the spectrum used had little variation. Measurements were performed to ascertain the stability of the output power level of the receiver. This output was found to be constant in all cases for periods much longer than the time required to make one measurement. A block diagram of the components used for this measurement is shown in Fig. 9. A 2K39 klystron was used as the local oscillator. Its output was fed through a frequency meter, tuner, and attenuator to a magic tee. Half the power was dissipated in a matched termination and the remaining half was coupled into one arm of the short slot hybrid section[3] where it was split equally between the two crystals. The power level was set so that one milliwatt of local oscillator power was available at each crystal. The output power of the 2K25 frequency modulated klystron was coupled from an attenuator to a coaxial cable so that it could be fed into either of two channels. In one case the output power

[3] H. Riblett, "Short slot hybrid section," Proc. I.R.E., vol.40, pp.180-184; February 1952.

was fed through a precision calibrated attenuator and "Uniline" (non-reciprocal attenuator) to a magic tee. Half this power was dissipated in the termination and the other half coupled to the short slot hybrid section from the same arm as the local oscillator. It is seen that the signal power present in the local oscillator arm of the balanced mixer is analogous to local oscillator noise. The magic tee was used to couple these signals, to assure that there be no interaction between the two.

Since the IF input transformer cancelled in-phase signals, the simulated noise signal was suppressed. Since the IF outputs initially were in phase because the signal was coupled in the same arm as the local oscillator, the IF signals (with respect to the local oscillator) will always be of the same phase. In the other case, the signal was coupled through a calibrated attenuator and "Uniline" to the other arm of the balanced mixer and was out of phase with respect to the local oscillator, thereby giving maximum IF output power. In this case, the 2K25 output power simulated signal power from an antenna. The pre-amplifier, communications receiver, detector, and output meter were used to amplify and detect this IF signal. It is readily seen from the above discussion that if the output meter reading is set at the same level for the two cases, the local oscillator noise suppression is simply the difference of the required attenuation in the two paths.

5. Correction for IF Unbalance

Since any unbalance in the two transformers would lead to erroneous results, a study of the effects and a possible correction for this unbalance is necessary. The two basic equations for local oscillator noise suppression derived previously are:

$$S_o = \left(\frac{1 + \frac{\sqrt{L_1}}{\sqrt{L_2}}}{1 - \frac{\sqrt{L_1}}{\sqrt{L_2}}} \right)^2$$

for the magic tee input circuit

$$S_o = \left(\frac{1 + \frac{I_{sc_1}}{I_{sc_2}}}{1 - \frac{I_{sc_1}}{I_{sc_2}}} \right)^2$$

for the non-magic tee input circuit

For either case if

$$a = \frac{\sqrt{L_1}}{\sqrt{L_2}} \text{ or } \frac{I_{sc_1}}{I_{sc_2}}$$

(a is defined as less than or equal to one), the true local oscillator noise suppression becomes

$$S_o = \left(\frac{1 + a}{1 - a}\right)^2 \tag{18}$$

The assumption is made that any unbalance in the input circuit can be accounted for by an unbalance factor K (experimental data, which will be discussed, shows this to be a good assumption). If this is true, then any unbalance would modify the above equation by a factor K (defined to be equal to or less than unity) such that the suppression would then be:

$$S_1 = \left(\frac{1 + aK}{1 - aK}\right)^2 \tag{19}$$

If the crystals were reversed in their holders the suppression would be

$$S_2 = \left(\frac{1 + a/K}{1 - a/K}\right)^2 \tag{20}$$

It is readily seen from the above measured values of S_1 and S_2 that the true suppression can be found by taking the geometric mean of the constants aK and a/K and substituting this value in Eq. 18. There are two possible solutions for S_o depending upon the magnitude of a/K. From Eq. 19, for $K < a$,

$$S_1^{\frac{1}{2}} = \frac{1 + aK}{1 - aK} \tag{21}$$

which becomes

$$aK = \frac{S_1^{\frac{1}{2}} - 1}{S_1^{\frac{1}{2}} + 1} \tag{22}$$

From Eq. (20)

$$-\left(S_2^{\frac{1}{2}}\right) = \frac{1 + a/K}{1 - a/K} \tag{23}$$

Solving for a/K

$$a/K = \frac{S_2^{\frac{1}{2}} + 1}{S_2^{\frac{1}{2}} - 1} \tag{24}$$

Taking the mean of (22) and (24) gives

$$a = \sqrt{\frac{(S_1^{\frac{1}{2}} - 1)\ (S_2^{\frac{1}{2}} + 1)}{(S_1^{\frac{1}{2}} + 1)\ (S_2^{\frac{1}{2}} - 1}} \tag{25}$$

from which S_0 is calculated by substituting this value of a in Eq. (18). Similarly for $K > a$,

$$a = \sqrt{\frac{(S_1^{\frac{1}{2}} - 1)\ (S_2^{\frac{1}{2}} - 1)}{(S_1^{\frac{1}{2}} + 1)\ (S_2^{\frac{1}{2}} + 1)}} \tag{26}$$

From the above equations a family of curves giving S_0 as a function of S_1 with S_2 as a parameter were plotted for $K < a$ and $K > a$ and are shown in Figs. 10 and 11, respectively. As a check upon the validity of the above correction curves, measurements were made on a group of crystal pairs which consisted of one 1N23B crystal and one 1N23BR crystal of reversed polarity. Using these pairs, noise suppression measurements were made using a single transformer. By reversing one crystal the polarity of the IF signal is reversed at that crystal. Therefore, the noise outputs are out of phase while the signal outputs are in phase. Since a simple transformer would then give the desired suppression, the local oscillator noise suppression measurements taken are therefore independent of unbalance in the IF circuit. Using these results as the true values of noise suppression, the noise suppression of the same crystal pairs using the push-pull type of IF circuit were measured. From the measured values of S_1 and S_2 the correction curves were used and the resulting S_0 was compared to the S_0 measured with one transformer. The push-pull transformer arrangement was deliberately unbalanced to obtain the most severe case where $K < a$. The results show excellent agreement between the two values of local oscillator noise suppression obtained for each pair, indicating that the method described for correcting IF unbalance is valid.

6. Experimental Results

Using this procedure for measuring local oscillator noise suppression which gives results that depend only on the degree of crystal balance, noise suppression of a large number of crystal pairs for both the magic tee and the non-magic tee IF circuits was studied. The results show conclusively that correlation with single ended measurements, is very good provided the correct equation for the type of IF circuit employed is used. Typical correlation curves for the two types of IF circuits are shown in Figs. 12 and 13. It is to be noted that the results were obtained for crystal pairs of arbitrary rf impedance phase. Thus, these data corroborate the theory. In obtaining the data for conversion loss and IF impedance, the rectified crystal current was also noted. The degree of correlation was not as definite as in the other cases. As a further check upon the results, measurements were made at 35,000 mc using 1N53 crystals. A photograph of the equipment used in this study is shown in Fig. 14. These results are very similar to those obtained in X band. They further demonstrated that local oscillator noise suppression is a function only of conversion loss and IF impedance of the crystal pair.

Acknowledgments

The authors wish to express their thanks to Mr. Abraham Boguslaw for his help in preparing the manuscript and to Mr. Irving Birnbaum for his over-all supervision and guidance.

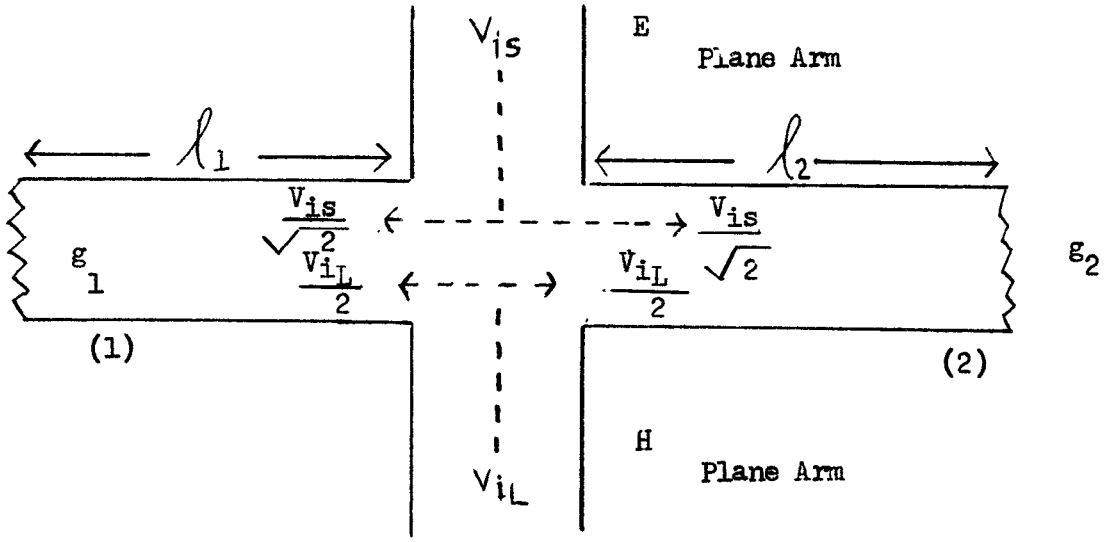

Fig. 1 - Equivalent rf circuit of magic tee balanced mixer.

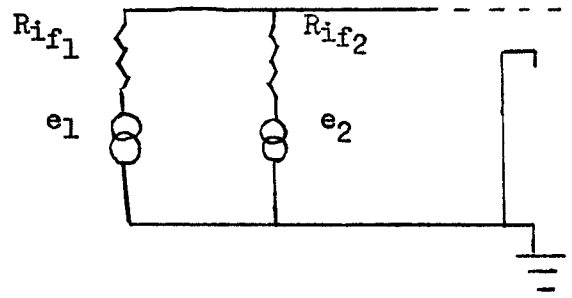

Fig. 2 - Equivalent IF output circuit as seen at the grid of the preamplifier.

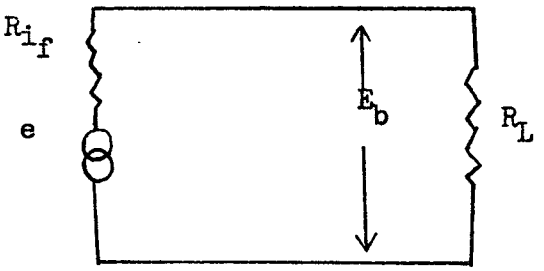

Fig. 3 - Equivalent output circuit of a conversion loss test set.

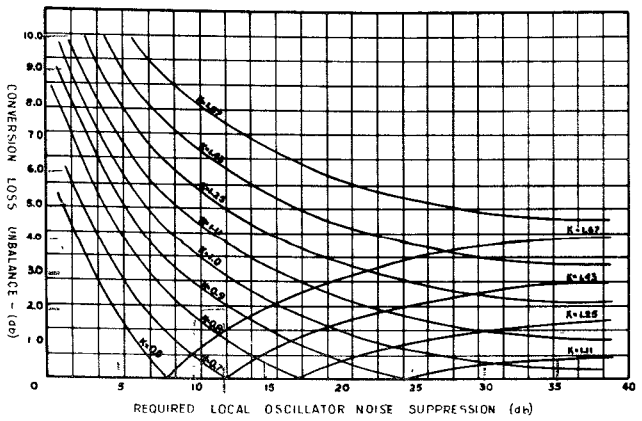

Fig. 4 - Curves of local oscillator noise suppression versus conversion loss unbalance with IF impedance unbalance as a parameter.

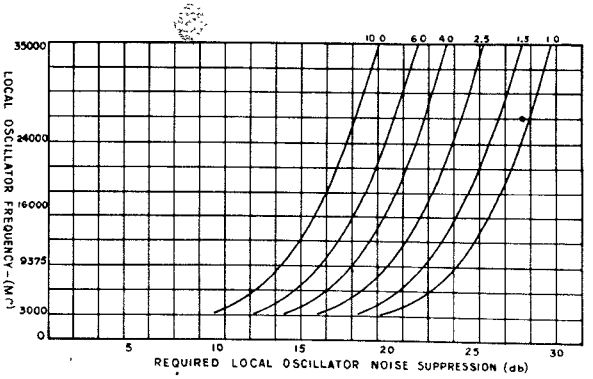

Fig. 5 - Curves of required local oscillator noise suppression versus frequency with $(t-1+F_{if})$ as a parameter for $\Delta F_{db} = 0.2$ db.

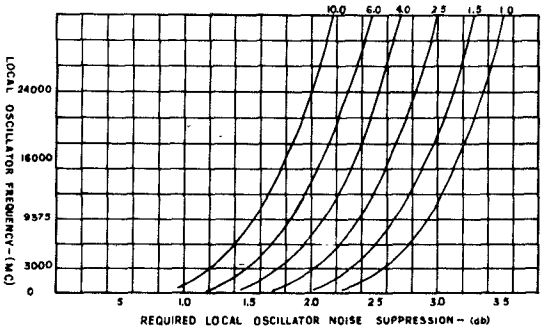

Fig. 6 - Curves of required local oscillator noise suppression versus frequency with $(t-1+F_{if})$ as a parameter for ΔF_{db} = ~~0.3~~ db.

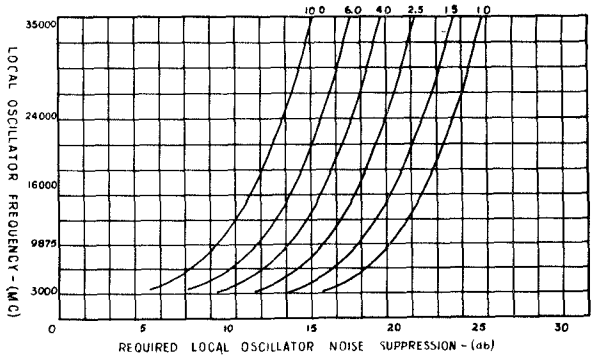

Fig. 7 - Curves of required local oscillator noise suppression versus frequency with $(t-1+F_{if})$ as a parameter for ΔF_{db} = 0.4 db.

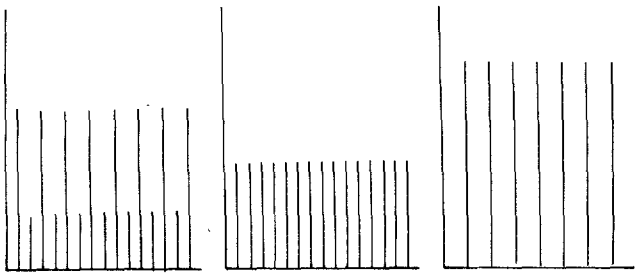

Fig. 8 - Possible klystron power spectra for different values of X.

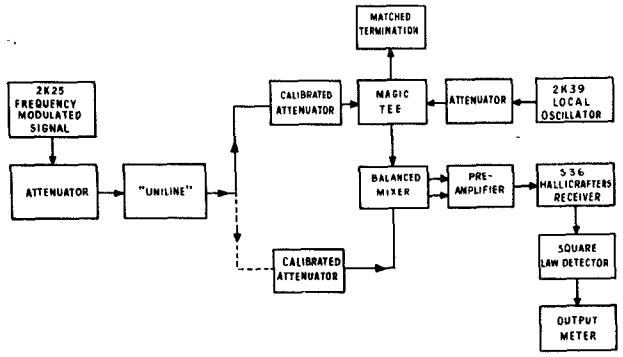

Fig. 9 - Block diagram for local oscillator noise suppression measurements in X band.

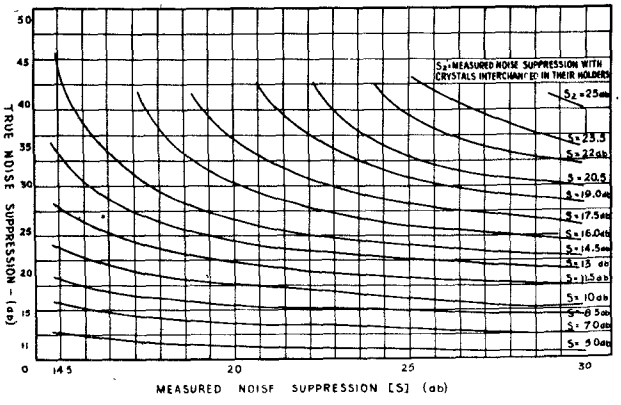

Fig. 10 - Correction curves for measurements under severe transformer unbalance.

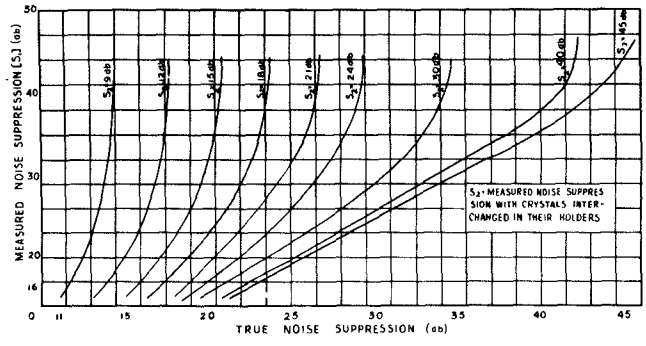

Fig. 11 - Correction curves for measurements under small transformer unbalance.

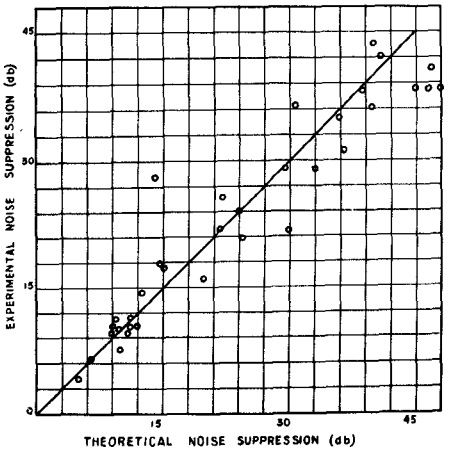

Fig. 12 - Correlation curve of noise suppression with magic tee IF circuit versus calculated values.

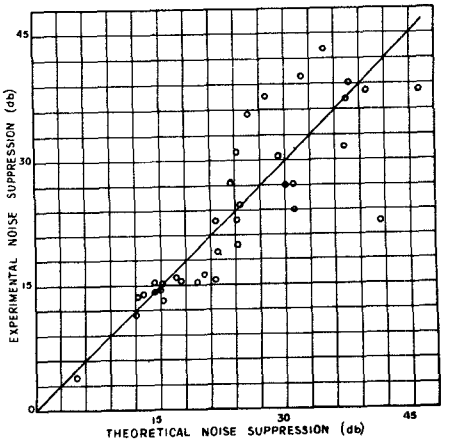

Fig. 13 - Correlation curve of noise suppression with non magic tee IF circuit versus calculated values.

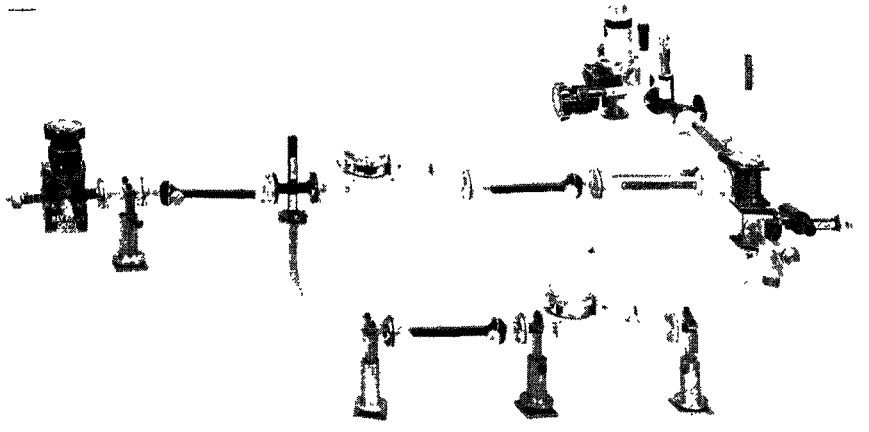

Fig. 14 - Microwave components employed at 35,000 mc for local oscillator noise suppression measurements.